

RECEIVED: March 27, 2019

REVISED: May 18, 2019

ACCEPTED: May 21, 2019

PUBLISHED: June 10, 2019

Matching for FCNC effects in the flavour-symmetric SMEFT

Tobias Hurth,^a Sophie Renner^a and William Shepherd^{a,b}

^a*PRISMA+ Cluster of Excellence & Mainz Institute of Theoretical Physics,
Johannes Gutenberg-Universität Mainz,
55099 Mainz, Germany*

^b*Physics Department, Sam Houston State University,
Huntsville, TX 77431, U.S.A.*

E-mail: hurth@uni-mainz.de, sorennen@uni-mainz.de, shepherd@shsu.edu

ABSTRACT: We calculate the complete tree and one-loop matching of the dimension-six Standard Model Effective Field Theory (SMEFT) with unbroken $U(3)^5$ flavour symmetry to the operators of the Weak Effective Theory (WET) which are responsible for flavour changing neutral current effects among down-type quarks. We also explicitly calculate the effects of SMEFT corrections to input observables on the WET Wilson coefficients, a necessary step on the way to a well-defined, complete prediction. These results will enable high-precision flavour data to be incorporated into global fits of the SMEFT at high energies, where the flavour symmetry assumption is widespread.

KEYWORDS: Beyond Standard Model, Effective Field Theories, Heavy Quark Physics

ARXIV EPRINT: [1903.00500](https://arxiv.org/abs/1903.00500)

Contents

1	Introduction	1
2	Flavour-symmetric SMEFT	3
3	Method and inputs	6
4	Results	9
4.1	$Q_{qq}^{(1)}$ and $Q_{qq}^{(3)}$	9
4.2	$Q_{lq}^{(1)}$, $Q_{lq}^{(3)}$, Q_{eu} , Q_{lu} and Q_{qe}	11
4.3	$Q_{Hl}^{(1)}$ and Q_{He}	11
4.4	$Q_{Hq}^{(1)}$ and Q_{Hu}	12
4.5	$Q_{Hq}^{(3)}$	12
4.6	Q_W	14
4.7	Q_{HWB}	14
4.8	Q_{HD}	14
4.9	$Q_{Hl}^{(3)}$ and Q_{ll}	15
5	Conclusions and outlook	16
A	Input parameter dependence of results	17
A.1	Input shift independent pieces	18
A.1.1	$Q_{Hl}^{(3)}$	18
A.1.2	Q_{HD}	18
A.1.3	C_{HWB}	18
A.2	Input shift pieces for $\{\hat{m}_W, \hat{m}_Z, \hat{G}_F\}$ scheme	19
A.3	Input shift pieces for $\{\hat{\alpha}_{em}, \hat{m}_Z, \hat{G}_F\}$ scheme	19

1 Introduction

Despite the historically impressive performance of the LHC, with massive datasets delivered at the highest collision energies ever achieved in a laboratory, an understanding of the nature of physics beyond the Standard Model (SM) remains elusive. Since the 2012 discovery of a Higgs-like scalar [1, 2] (whose properties continue to look more and more Higgs-like with increasing scrutiny [3, 4]), the SM has been completed, but the questions left unanswered by it remain as compelling as ever.

In the face of this uncertainty as to the nature of whatever new physics (NP) underlies the SM at higher energy scales, it makes sense to remain as agnostic as possible in our interpretations of the data that is available to us. This will allow us to make accurate

statements which apply not only to the particular theories which are *en vogue* at the moment, but also to theories which have not yet been dreamt up. In the interest of enabling such an agnostic analysis of physics data, the SM Effective Field Theory (SMEFT) (for a recent review see [5]) is an essential tool. This provides the technology for defining a basis of interaction types which, under the assumption that $h(125)$ is the remnant of the electroweak doublet responsible for electroweak symmetry breaking, spans the full set of possibilities that could be induced by NP when probed below its characteristic energy scale, which we denote as Λ . An analysis framed in terms of the operators of the SMEFT can be straightforwardly mapped into constraints on an arbitrary model of heavy NP using the well-understood technology of amplitude matching, now possible using various automated tools [6, 7]. The interface between different codes, and translation between operator bases, is facilitated by the Wilson coefficient exchange format initiative [8].

Many steps toward the implementation of SMEFT as a target for analysis have already been taken. The appropriate theoretical underpinnings of the SMEFT theory itself have been developed, notably the determination of a complete basis of operators at dimension-six [9] and their renormalization [10–12]. Precision electroweak data have been used to develop fits of the relevant subset of operators that contribute to those observables [13–19]. Loop corrections to very precisely measured and particularly interesting processes have been calculated [20–32]. LHC searches have also been interpreted in the SMEFT, with techniques to address the unique theoretical errors inherent in high energy searches for EFT effects recently developed [33, 34]. Ultimately, all of these contributions will need to coalesce into a fully global fit of the SMEFT Wilson coefficients and cutoff scale, as only then will it be possible to truly understand the conservative constraints which can be imposed on an arbitrary model through matching to the SMEFT and comparison of a given parameter point to the likelihood associated with all the relevant measurements.

An important source of precise data which should be used as much as possible is the output of the tremendous effort of the experimental flavour physics community, where measurements of a vast number of processes have been made, nearly all of which indicate that the approximate flavour symmetry which is present in the SM must remain very nearly correct up to scales far higher than we typically expect of NP. Many groups have studied the implications of the SMEFT for flavour observables and vice versa (e.g. [35–57]), often focussing on subsets of operators which contribute to particular vertices, or considering explicitly flavour-violating interactions within the SMEFT itself. Codes also exist to perform the running above and below the electroweak scale, and the tree level matching between the SMEFT and the WET [58, 59].

Here, we tackle the problem with a symmetry-led approach. Taking as a starting point the observation that large flavour violating effects beyond the Standard Model are already ruled out, but retaining the hope of NP at the TeV scale (which could, for instance, address the gauge hierarchy problem), we begin from the simple assumption of an exact flavour symmetry (a particularly strong case of Minimal Flavour Violation [60]), and include in our theory all operators which are invariant under this. In this article we present the full tree and one-loop matching between the CP conserving, $U(3)^5$ -symmetric SMEFT at dimension-six and down type flavour-changing neutral current operators in the weak

effective theory (WET) which arises when the heavy gauge bosons, Higgs boson, and top quark are integrated out of the theory. Flavour violation is due purely to SM effects in the CKM matrix describing the interactions of W^\pm bosons with the quarks.

These calculations of the loop effects of flavour conserving operators may be relevant even in cases where this symmetry is not imposed *ab initio*, when the tree-level flavour changing effects are required to be sufficiently suppressed that loop-level contributions from flavour-symmetric or flavourless couplings become comparable to them. Furthermore, most global fits to SMEFT coefficients using LEP and LHC data have been performed assuming this flavour-symmetric paradigm, so exploring this parameter region in detail in the flavour sector will allow for additional observables to be included in these fits, leading to new and/or tighter constraints. Finally, this assumption represents a “worst-case scenario” for flavour searches in the context of roughly TeV-scale NP, so this calculation will give an insight into the smallest effects we should reasonably expect to see if NP is near the TeV scale.

An additional important feature of this article is its inclusion of the non-trivial effects of the SMEFT on observables used as inputs to define Lagrangian parameters [14, 61]. In order to make a physical prediction of an observable in quantum field theory it is necessary to define all of the Lagrangian parameters of the theory in terms of observables. In the SM these definitions are so long standing, and the observables used so standardized, that we have grown used to simply assigning numerical values to the Lagrangian parameters as though they were measured themselves, but this is not the case. The SMEFT is not turned on only for “signal” processes and inactive in “input” measurements; its effects on both measurements must be considered in order to properly predict the sensitivity of any observable to the Wilson coefficients parameterizing new physics effects.

In the next section, we shall discuss the particular set of interactions that arise in the flavour-symmetric limit of the SMEFT. In section 3 we lay out our methods and explain how we fix free parameters in the SMEFT Lagrangian using measurements of input parameters. Then, in section 4 we present the results of our matching calculation between the SMEFT and WET, considering in turn direct contributions from new coupling structures in the SMEFT not present in the SM and contributions from SMEFT effects on the extraction of would-be SM couplings from experimental input measurements. We conclude in section 5 with a discussion of the implications and utility of this matching calculation, as well as a mention of future directions. The input dependence of our results is explained in appendix A, where we provide a separation of the calculation into pieces that are independent of the input parameters chosen, and pieces that arise purely due to SMEFT effects in input parameter measurements, given in two different input schemes.

2 Flavour-symmetric SMEFT

The SMEFT formalism expands upon the structure of the SM by allowing for additional, non-renormalizable operators. This introduces an additional perturbation series to the theory, expanding in inverse powers of the energy scale characterizing the new BSM physics, and an appropriate choice of expansion order must be made for both this new series as well as the usual series in gauge and Yukawa couplings already present in the SM. In

Group	Operators	$d_i \rightarrow d_j \gamma$	$d_i \rightarrow d_j l^+ l^-$	Meson mixing
1	Q_G	-	-	-
	Q_W	✓	✓	-
2	Q_H	-	-	-
3	$Q_{H\Box}$	-	-	-
	Q_{HD}	✓	✓	-
4	Q_{HG}	-	-	-
	Q_{HW}	-	-	-
	Q_{HB}	-	-	-
	Q_{HWB}	✓	✓	-
7	$Q_{H\ell}^{(1)}$	-	✓	-
	$Q_{H\ell}^{(3)}$	✓*	✓	✓*
	Q_{He}	-	✓	-
	$Q_{Hq}^{(1)}$	-	✓	-
	$Q_{Hq}^{(3)}$	✓	✓	✓
	Q_{Hu}	-	✓	-
	Q_{Hd}	-	-	-

Table 1. All operators with 2 or fewer fermions that are invariant under CP and the $U(3)^5$ flavour symmetry. Ticks indicate that they contribute to the FCNC processes we consider. An asterisk (*) signifies that the contribution is only indirect, via effects in input parameter measurements.

this article we shall keep only the first non-trivial BSM contribution to the observables considered, which occurs at order $1/\Lambda^2$, where Λ is again the new physics scale.

We choose to work with the Warsaw basis [9] of dimension-6 operators for our calculations; this basis is particularly well suited to a loop-level calculation as higher-derivative operators have been systematically removed in its construction, and it is the only basis whose complete renormalization behaviour is known [10–12]. The full basis is given in the appendix in table 3; we shall refer to operators by the names given in that table throughout the article, and denote the Wilson coefficient of operator Q_a as C_a .

We select operators by starting from a $U(3)^5$ flavour symmetry defined as

$$U(3)_q \times U(3)_u \times U(3)_d \times U(3)_l \times U(3)_e, \tag{2.1}$$

and under which the SM fermion fields have charges

$$\begin{aligned} q &\sim (3, 1, 1, 1, 1), & u &\sim (1, 3, 1, 1, 1), & d &\sim (1, 1, 3, 1, 1), \\ l &\sim (1, 1, 1, 3, 1), & e &\sim (1, 1, 1, 1, 3). \end{aligned} \tag{2.2}$$

We are considering only the effects of flavour symmetric operators here, meaning operators which are overall singlets under the $U(3)^5$ symmetry. Many operators are straightforwardly

Group	Operators	$d_i \rightarrow d_j \gamma$	$d_i \rightarrow d_j l^+ l^-$	Meson mixing
8: $(\bar{L}L)(\bar{L}L)$	$Q_{\ell\ell}$	✓*	✓*	✓*
	$Q_{qq}^{(1)}$	-	✓	✓
	$Q_{qq}^{(3)}$	-	✓	✓
	$Q_{lq}^{(1)}$	-	✓	-
	$Q_{lq}^{(3)}$	-	✓	-
8: $(\bar{R}R)(\bar{R}R)$	Q_{ee}	-	-	-
	Q_{uu}	-	-	-
	Q_{dd}	-	-	-
	Q_{eu}	-	✓	-
	Q_{ed}	-	-	-
	$Q_{ud}^{(1)}$	-	-	-
	$Q_{ud}^{(8)}$	-	-	-
8: $(\bar{L}L)(\bar{R}R)$	$Q_{\ell e}$	-	-	-
	$Q_{\ell u}$	-	✓	-
	$Q_{\ell d}$	-	-	-
	Q_{qe}	-	✓	-
	$Q_{qu}^{(1)}$	-	-	-
	$Q_{qu}^{(8)}$	-	-	-
	$Q_{qd}^{(1)}$	-	-	-
	$Q_{qd}^{(8)}$	-	-	-

Table 2. All four-fermion operators that are invariant under CP and the $U(3)^5$ flavour symmetry. Ticks indicate that they contribute to the FCNC processes we consider. An asterisk (*) signifies that the contribution is only indirect, via effects in input parameter measurements.

forbidden from our analysis by this requirement; all the operators of classes 5 and 6 violate the flavour symmetry ansatz, as do the scalar-scalar interactions in class 8, and the operator Q_{Hud} . All operators which are invariant under CP and the $U(3)^5$ flavour symmetry are listed in tables 1 and 2, where we also indicate which down-type FCNC processes are affected by each operator at one loop.

In the interest of compactness, we define the Wilson coefficients in the SMEFT to be dimensionful throughout, such that the dimension-six Lagrangian terms are written simply as

$$\mathcal{L}_6 = \sum_a C_a Q_a. \quad (2.3)$$

We drop flavour indices throughout our calculation, as our flavour symmetry assumption leads to the insistence that all the Wilson coefficient matrices in flavour space are identity-like, with the interesting exception of current-current four-fermion interactions of identical

currents. Only three operators of that type contribute in our calculation: Q_{ll} and $Q_{qq}^{(1)}$ contribute solely in the “off-diagonal” flavour combination which reads $\delta_{pt}\delta_{rs}$, and $Q_{qq}^{(3)}$ contributes in both allowed flavour combinations. The Wilson coefficients of the “identity-like” combination $\delta_{pr}\delta_{st}$ is denoted here unprimed ($C_{qq}^{(3)}$, $C_{qq}^{(1)}$, C_{ll}), while those of the “off-diagonal” combinations are primed ($C_{qq}^{(3)'}$, $C_{qq}^{(1)'}$, C_{ll}').

In addition to restricting ourselves to the leading-order contributions in the new, EFT perturbation expansion, we shall also restrict our attention to contributions which arise at one-loop order (at most) in the SMEFT. Given the flavour assumptions we have made, there are no tree-level contributions to FCNC processes, with the exception of those arising from $Q_{qq}^{(1,3)}$. The fact that $Q_{qq}^{(1,3)}$ contain two quark currents make these the only operators that can mediate down-type quark flavour changing currents at tree level — even if their Wilson coefficients are diagonal in the flavour basis — due to the misalignment between the up- and down-type quark mass matrices characterised by the CKM. Upon rotating to the mass basis, therefore, interactions of the form $V_{ij}V_{kl}^*(\bar{u}_i^\alpha\gamma_\mu P_L d_j^\alpha)(\bar{u}_k^\beta\gamma_\mu P_L d_l^\beta)$ or $V_{ij}V_{kl}^*(\bar{u}_i^\alpha\gamma_\mu P_L d_j^\beta)(\bar{u}_k^\beta\gamma_\mu P_L d_l^\alpha)$ (where α, β are colour indices) are induced from these flavour singlet operators, similarly to the effect of integrating out the W^\pm boson between two quark currents in the SM. In the vast majority of cases, though, the leading-order contribution of the SMEFT to FCNC processes starts at one loop under our assumptions. This is in contrast to the analysis of ref. [43], in which the SMEFT Wilson coefficients were considered in more generality, allowing most operators containing down-type quarks to contribute to $d_i \rightarrow d_j$ transitions at tree level. Hence ref. [43] presents loop-level matching results only for operators containing a right-handed up type quark (some of which are excluded from our analysis since they are not $U(3)^5$ flavour singlets). These differing approaches ensure that many of the matching calculations presented here are new, but we compare with and refer to existing results in the literature wherever possible.

In the following we focus on $b \rightarrow s$ FCNC transitions for concreteness of notation, but (since the theory is flavour symmetric) our calculation applies equally well to $b \rightarrow d$ or $s \rightarrow d$ transitions as well, with the appropriate generation index replacements. Our goal in performing this calculation is to enable one-loop studies of the effects of flavour-symmetric SMEFT on down-type FCNC leptonic, semi-leptonic, or photonic decays and $\Delta F = 2$ meson oscillations. We neglect loop-level matching to operators which only affect these processes via mixing, which leads to an additional suppression.

3 Method and inputs

Before embarking on the matching calculations, a choice must be made about which measurements to use to fix the free parameters of the theory. Measurements of inputs, for example the Fermi constant G_F , may be polluted by the effects of dimension-six operators in the SMEFT. Other dimension-six operators produce new contributions to the masses and mixings of gauge bosons and fermions when the Higgs takes its vev. Hence the coefficients of these operators will have knock-on effects wherever the inputs enter into other calculations. The input choice is especially important in the electroweak sector of the theory, where the presence of the operators Q_{HD} and Q_{HWB} breaks the usual SM relations

between the Lagrangian parameters v , g_1 , g_2 , $\sin\theta$, m_W and m_Z . These issues have been discussed at length in the literature (see e.g. [13, 14, 61–63]).

In the main text of this paper, we present our results in a scheme in which the set of input measurements are

$$\left\{ \hat{m}_W, \hat{m}_Z, \hat{G}_F, \hat{m}_t, \hat{m}_b, \hat{\alpha}_s, \hat{V}_{CKM} \right\}. \quad (3.1)$$

We denote these measured inputs, as well as parameters derived from them via SM relations, with a hat [61]:

$$\begin{aligned} \hat{v} &= \frac{1}{2^{1/4}\sqrt{\hat{G}_F}}, & \hat{g}_1 &= 2 \cdot 2^{1/4}\hat{m}_Z\sqrt{\hat{G}_F\left(1 - \frac{\hat{m}_W^2}{\hat{m}_Z^2}\right)}, & \hat{g}_2 &= 2 \cdot 2^{1/4}\hat{m}_W\sqrt{\hat{G}_F}, \\ \hat{y}_t &= \frac{\sqrt{2}\hat{m}_t}{\hat{v}}, & \hat{y}_b &= \frac{\sqrt{2}\hat{m}_b}{\hat{v}}, & \hat{g}_s &= \sqrt{4\pi\hat{\alpha}_s}. \end{aligned} \quad (3.2)$$

Within our $U(3)^5$ flavour assumption, the mapping from the measured inputs $\hat{\alpha}_s$ and \hat{V}_{CKM} to Lagrangian parameters goes through similarly to in the SM. However, things are slightly less trivial for the electroweak sector. In this case there are three free Lagrangian parameters, which we take to be the gauge couplings \bar{g}_1 and \bar{g}_2 , and the electroweak vev \bar{v} , where the bars indicate that these are SMEFT Lagrangian parameters. Once these are fixed by solving for the input measurements \hat{G}_F , \hat{m}_W and \hat{m}_Z , they can be written as the sum of the respective hatted parameters and a shift which depends on SMEFT dimension-six Wilson coefficients:

$$\begin{aligned} \bar{g}_1 &= \hat{g}_1 + \delta g_1, \\ \bar{g}_2 &= \hat{g}_2 + \delta g_2, \\ \bar{v} &= \hat{v} + \delta v. \end{aligned} \quad (3.3)$$

For our choice of inputs, the operators that enter into the shifts δg_1 , δg_2 and δv are C_{HWB} , C_{HD} , $C_{HI}^{(3)}$ and C'_H . Then the procedure for deriving the Feynman rules can be understood via the following steps:

1. Write the Lagrangian in terms of canonically normalised mass eigenstates, and the three free electroweak parameters (\bar{g}_1 , \bar{g}_2 , \bar{v})
2. Derive Feynman rules in terms of these three parameters
3. Write the free parameters in terms of measured inputs and the dimension-six shifts (δg_1 , δg_2 and δv) and substitute them into Feynman rules, consistently retaining terms of order $1/\Lambda^2$

Steps 1 and 2 have been done in ref. [64], and step 3 can be trivially performed from the Feynman rules in that reference using eqs. (3.3), and remembering that the gauge boson

masses in the SMEFT are¹

$$m_W^2 = \frac{\bar{g}_2^2 \bar{v}^2}{4}, \quad (3.4)$$

$$m_Z^2 = \frac{\bar{v}^2}{4} (\bar{g}_1^2 + \bar{g}_2^2) + \frac{1}{8} \bar{v}^4 C_{HD} (\bar{g}_1^2 + \bar{g}_2^2) + \frac{1}{2} \bar{v}^4 \bar{g}_1 \bar{g}_2 C_{HWB}. \quad (3.5)$$

Since the measured quark masses \hat{m}_t and \hat{m}_b are taken as inputs, the Yukawa couplings \bar{y}_t and \bar{y}_b are affected by the shift δv as

$$\bar{y}_t = \sqrt{2} \frac{\hat{m}_t}{\bar{v}} = \hat{y}_t (1 - \delta v), \quad (3.6)$$

$$\bar{y}_b = \sqrt{2} \frac{\hat{m}_b}{\bar{v}} = \hat{y}_b (1 - \delta v). \quad (3.7)$$

All other fermion masses are set to zero in our calculation.² We provide more explicit details of the procedure — including the expressions for δg_1 , δg_2 and δv , as well as quoting our results in a different scheme in which $\{\hat{\alpha}_{em}, \hat{m}_Z, \hat{G}_F\}$ are the electroweak inputs — in appendix A.

The WET effective Hamiltonian for $\Delta B = \Delta S = 1$ transitions to which the symmetric SMEFT matches is identical to the WET basis of the SM. This is a consequence of our flavour symmetry assumption.

$$\mathcal{H}_{\text{eff}}^{|\Delta B|=|\Delta S|=1} = \frac{4\hat{G}_F}{\sqrt{2}} \left[-\frac{1}{(4\pi)^2} \hat{V}_{ts}^* \hat{V}_{tb} \sum_{i=3}^{10} C_i \mathcal{O}_i + \sum_{q=u,c} \hat{V}_{qs}^* \hat{V}_{qb} (C_1 \mathcal{O}_1^q + C_2 \mathcal{O}_2^q) \right], \quad (3.8)$$

with

$$\begin{aligned} \mathcal{O}_1^q &= (\bar{b}^\alpha \gamma_\mu P_L q^\beta) (\bar{q}^\beta \gamma^\mu P_L s^\alpha), \\ \mathcal{O}_2^q &= (\bar{b}^\alpha \gamma_\mu P_L q^\alpha) (\bar{q}^\beta \gamma^\mu P_L s^\beta), \\ \mathcal{O}_7 &= \hat{e} \hat{m}_b (\bar{s} \sigma^{\mu\nu} P_R b) F_{\mu\nu}, \\ \mathcal{O}_8 &= \hat{g}_s \hat{m}_b (\bar{s} \sigma^{\mu\nu} T^A P_R b) G_{\mu\nu}^A, \\ \mathcal{O}_9 &= \hat{e}^2 (\bar{s} \gamma^\mu P_L b) (\bar{\ell} \gamma_\mu \ell), \\ \mathcal{O}_{10} &= \hat{e}^2 (\bar{s} \gamma^\mu P_L b) (\bar{\ell} \gamma_\mu \gamma_5 \ell). \end{aligned} \quad (3.9)$$

where α, β are colour indices. For the definition of the QCD penguin operators $\mathcal{O}_{3,4,5,6}$ we refer to ref. [65]. In the SM, C_2 receives tree level contributions, while C_{3-10} are generated only at loop level. We will find that our flavour symmetry assumption ensures that a similar matching pattern arises in the SMEFT, although we additionally get a tree level contribution to C_1 . As discussed before, we neglect loop-level matching to four-quark operators, since their effects in these processes is only via mixing and, thus, are suppressed compared to the direct one-loop matching contributions to $C_7 - C_{10}$.

¹For derivations of these see e.g. ref. [12].

²With the exception of including leading charm mass effects in meson mixing coefficients, for application to kaon mixing.

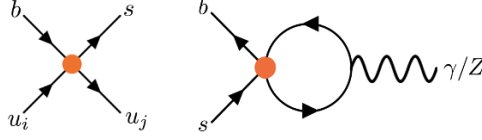


Figure 1. Diagrams generating contributions to the 4-quark WET coefficients $C_{1,2}$ (left) and to $b \rightarrow sl^+l^-$ (right) from the SMEFT operators $Q_{qq}^{(1)}$ and $Q_{qq}^{(3)}$.

The WET effective Hamiltonian for $\Delta B = \Delta S = 2$ transitions is again identical to the WET basis of the SM,

$$\mathcal{H}_{\text{eff}}^{|\Delta B|=|\Delta S|=2} = \frac{\hat{G}_F^2 \hat{m}_W^2}{16\pi^2} (\bar{s}_L^\alpha \gamma^\mu b_L^\alpha) (\bar{s}_L^\beta \gamma^\mu b_L^\beta) \times (\lambda_t^2 C_{1,mix}^s(x_t) + \lambda_c^2 C_{1,mix}^s(x_c) + 2\lambda_c \lambda_t C_{1,mix}^s(x_t, x_c)), \quad (3.10)$$

where α and β are colour indices, and $\lambda_i = \hat{V}_{is}^* \hat{V}_{ib}$. The coefficients $C_{1,mix}^s$ are functions of $x_i = m_i^2/m_W^2$, and only the first term $\lambda_t^2 C_{1,mix}^s(x_t)$ is non-negligible in the case of B_s (and B_d) mixing. However we include the functions $C_{1,mix}^s(x_c)$ and $C_{1,mix}^s(x_t, x_c)$ here — and quote their values (to linear order in $x_c \ll 1$) in the main text — to allow application of our matching results via trivial flavour index replacements to kaon mixing, where these terms are important.

4 Results

In this section we present our results for the matching of the $U(3)^5$ flavour and CP symmetric SMEFT theory onto the coefficients of the WET. All WET Wilson coefficients are at the electroweak scale m_W . We define Wilson coefficients in the SMEFT at the arbitrary scale μ and do not resum the logarithmic divergences of form $\log\left(\frac{\mu}{m_W}\right)$, leaving them explicit in our calculation for comparison with the anomalous dimension matrix of [10–12], with which we find agreement. We separate our results by SMEFT operator, or groups of similar operators, and we only present non-zero results. Our calculations have been done in R_ξ gauge using dimensional regularisation and we use the \overline{MS} prescription to remove divergences. In all cases we have confirmed that the separate contributions calculated here are gauge parameter independent. Where possible, we compare our results to those obtained previously in the literature. In all diagrams, orange blobs represent insertions of SMEFT operators, and unlabelled internal fermion lines are $u/c/t$ quarks.

To first order in $1/\Lambda^2$, the barred and hatted parameters (e.g. \bar{g}_1, \hat{g}_1 as introduced in section 3) are equal when they are multiplied by a SMEFT Wilson coefficient, so in the following we simply drop the hats and bars for simplicity. However we emphasise that the results presented here include the effects of input parameter shifts, and we are taking $\{m_W, m_Z, G_F\}$ as the set of electroweak input parameters, as explained in section 3.

4.1 $Q_{qq}^{(1)}$ and $Q_{qq}^{(3)}$

These are the only operators in our theory which generate a contribution to the $b \rightarrow s$ transition at tree level, shown in figure 1. As mentioned in section 2, there are two ways

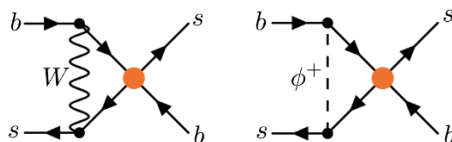


Figure 2. Diagrams generating contributions to B_s mixing from the SMEFT operators $Q_{qq}^{(1)}$ and $Q_{qq}^{(3)}$.

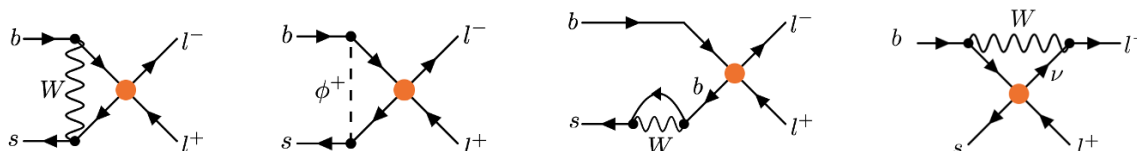


Figure 3. Diagrams generating contributions to $b \rightarrow sl^+l^-$ from Q_{eu} and Q_{lu} (first two diagrams only), $Q_{lq}^{(1)}$ and Q_{qe} (first three diagrams and similar) and $Q_{lq}^{(3)}$ (all four diagrams and similar).

of contracting the quark doublets to make a flavour singlet in both operators, so we can define four independent Wilson coefficients, $C_{qq}^{(3)}$, $C_{qq}^{(3)'}$, $C_{qq}^{(1)}$ and $C_{qq}^{(1)'}$, within our $U(3)^5$ invariant theory.

The contribution to the coefficients of the 4-quark WET operators \mathcal{O}_1 and \mathcal{O}_2 is

$$C_1 = v^2(C_{qq}^{(3)'} - C_{qq}^{(1)'}), \quad (4.1)$$

$$C_2 = -2v^2 C_{qq}^{(3)}. \quad (4.2)$$

Contributions to C_9 and C_{10} are generated by the second diagram of figure 1. We find

$$C_9 = -v^2 C_{qq}^{(3)} \left(\frac{8}{9} + \frac{x_t}{2} \frac{1 - 4s_\theta^2}{s_\theta^2} \right) \left(1 + \log \frac{m_t^2}{\mu^2} \right) + v^2 N_c (C_{qq}^{(3)'} - C_{qq}^{(1)'}) \left(\frac{4}{9} + \frac{x_t}{4} \frac{1 - 4s_\theta^2}{s_\theta^2} \right) \log \frac{m_t^2}{\mu^2}, \quad (4.3)$$

$$C_{10} = \frac{1}{2} \frac{1}{s_\theta^2} v^2 C_{qq}^{(3)} x_t \left(1 + \log \frac{m_t^2}{\mu^2} \right) - \frac{N_c}{4} \frac{1}{s_\theta^2} v^2 (C_{qq}^{(3)'} - C_{qq}^{(1)'}) x_t \log \frac{m_t^2}{\mu^2}. \quad (4.4)$$

where $N_c = 3$ is the number of QCD colours. These operators also generate contributions to B_s mixing from the diagrams in figure 2. These give

$$C_{1,\text{mix}}^s(x_t) = -v^2 \left(2C_{qq}^{(3)} + (C_{qq}^{(1)'} - C_{qq}^{(3)'}) \right) x_t, \quad (4.5)$$

$$C_{1,\text{mix}}^s(x_c) = -v^2 \left(2C_{qq}^{(3)} + (C_{qq}^{(1)'} - C_{qq}^{(3)'}) \right) x_c, \quad (4.6)$$

$$C_{1,\text{mix}}^s(x_t, x_c) = v^2 \left(2C_{qq}^{(3)} + (C_{qq}^{(1)'} - C_{qq}^{(3)'}) \right) x_c \log \frac{x_c}{x_t}. \quad (4.7)$$

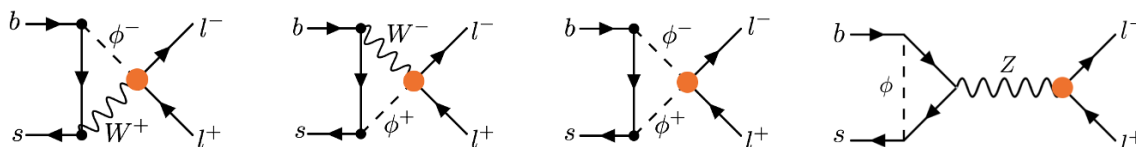


Figure 4. Diagrams generating contributions to $b \rightarrow sl^+l^-$ from $Q_{Hl}^{(1)}$ and Q_{He} operators. The fourth diagram should be taken to include all other Z penguin diagrams (including those with self-energies on external legs) where these operators affect the Zl^+l^- vertex.

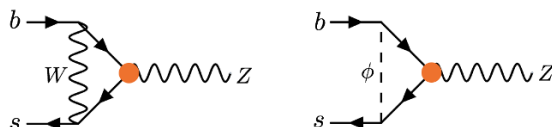


Figure 5. Diagrams generating contributions to $b \rightarrow sl^+l^-$ from $Q_{Hq}^{(1)}$ and Q_{Hu} operators.

4.2 $Q_{lq}^{(1)}$, $Q_{lq}^{(3)}$, Q_{eu} , Q_{lu} and Q_{qe}

These four-fermion operators contribute to $b \rightarrow sl^+l^-$ processes via the diagrams shown in figure 3. The contributions are

$$C_9 = \frac{v^2}{s_\theta^2} (C_{eu} + C_{lu} - C_{lq}^{(1)} - C_{qe}) I(x_t) - \frac{v^2}{s_\theta^2} C_{lq}^{(3)} I^{lq}(x_t), \quad (4.8)$$

$$C_{10} = \frac{v^2}{s_\theta^2} (C_{eu} - C_{lu} + C_{lq}^{(1)} - C_{qe}) I(x_t) + \frac{v^2}{s_\theta^2} C_{lq}^{(3)} I^{lq}(x_t), \quad (4.9)$$

where

$$I(x_t) = \frac{x_t}{16} \left[-\log \frac{m_W^2}{\mu^2} + \frac{x_t - 7}{2(1-x_t)} - \frac{x_t^2 - 2x_t + 4}{(1-x_t)^2} \log x_t \right], \quad (4.10)$$

$$I^{lq}(x_t) = \frac{x_t}{16} \left[-\log \frac{m_W^2}{\mu^2} + \frac{1 - 7x_t}{2(1-x_t)} - \frac{x_t^2 - 2x_t + 4}{(1-x_t)^2} \log x_t \right]. \quad (4.11)$$

Our results for C_{eu} and C_{lu} are in agreement with ref. [43].

4.3 $Q_{Hl}^{(1)}$ and Q_{He}

These operators produce effects in $b \rightarrow sl^+l^-$ via the diagrams shown in figure 4, giving

$$C_9 = -\frac{v^2}{s_\theta^2} (C_{Hl}^{(1)} + C_{He}) I(x_t), \quad (4.12)$$

$$C_{10} = \frac{v^2}{s_\theta^2} (C_{Hl}^{(1)} - C_{He}) I(x_t), \quad (4.13)$$

where $I(x_t)$ is defined in eq. (4.10).

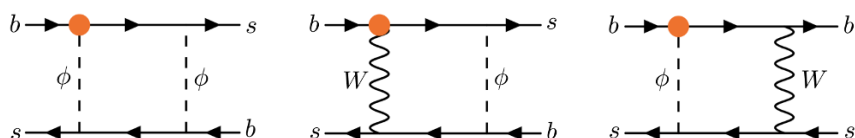


Figure 6. Diagrams generating contributions to B_s mixing from the $Q_{Hq}^{(3)}$ operator. Diagrams related to these by symmetry, as well as diagrams in which the operator connects to an s quark leg rather than a b quark leg, should be taken to be included.

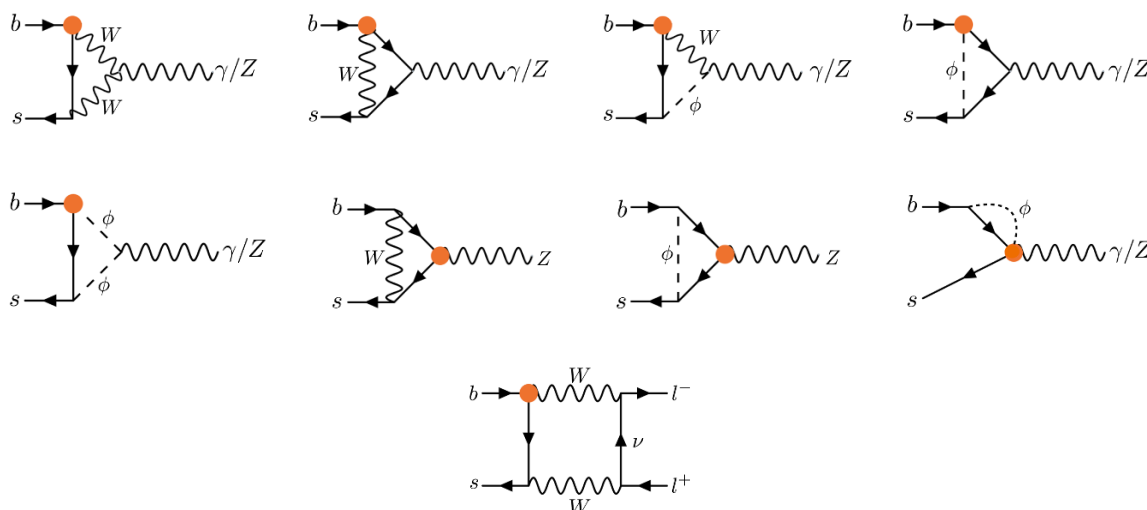


Figure 7. Diagrams generating contributions to $b \rightarrow sl^+l^-$ and/or $b \rightarrow s\gamma$ from the $Q_{Hq}^{(3)}$ operator. Diagrams in which the operator attaches to the b quark leg imply also the existence (and inclusion in our calculations) of similar diagrams with the operator attached to the s quark leg.

4.4 $Q_{Hq}^{(1)}$ and Q_{Hu}

These operators effectively just change the $Z\bar{u}_i u_i$ coupling and hence only enter in the Z penguin diagrams shown in figure 5. The contributions are

$$C_9 = v^2 \frac{(1 - 4s_\theta^2)}{s_\theta^2} (C_{Hu} - C_{Hq}^{(1)}) I(x_t), \tag{4.14}$$

$$C_{10} = \frac{v^2}{s_\theta^2} (C_{Hu} - C_{Hq}^{(1)}) I(x_t), \tag{4.15}$$

where $I(x_t)$ is defined in eq. (4.10). The C_{Hu} result is in agreement with ref. [43].

4.5 $Q_{Hq}^{(3)}$

This operator generates contributions to B_s mixing via the diagrams in figure 6, and to $b \rightarrow s\gamma$ and $b \rightarrow sl^+l^-$ via the diagrams in figure 7. There are also contributions to the chromomagnetic dipole operator via graphs similar to the second and fourth diagrams in figure 7, with a gluon replacing the photon. The Wilson coefficients of the mixing operator

and the (chromo)magnetic dipole operators are simple scalings of the SM result:

$$C_{1,\text{mix}}^s(x_t) = 4v^2 C_{Hq}^{(3)} S_0(x_t), \quad (4.16)$$

$$C_{1,\text{mix}}^s(x_c) = 4v^2 C_{Hq}^{(3)} S_0(x_c), \quad (4.17)$$

$$C_{1,\text{mix}}^s(x_t, x_c) = 4v^2 C_{Hq}^{(3)} S_0(x_t, x_c), \quad (4.18)$$

$$C_7 = -v^2 C_{Hq}^{(3)} D'_0(x_t), \quad (4.19)$$

$$C_8 = -v^2 C_{Hq}^{(3)} E'_0(x_t). \quad (4.20)$$

where

$$D'_0(x_t) = \frac{8x_t^3 + 5x_t^2 - 7x_t}{12(x_t - 1)^3} + \frac{x_t^2(2 - 3x_t)}{2(1 - x_t)^4} \log x_t, \quad (4.21)$$

$$E'_0(x_t) = \frac{x_t(x_t^2 - 5x_t - 2)}{4(x_t - 1)^3} + \frac{3}{2} \frac{x_t^2}{(x_t - 1)^4} \log x_t, \quad (4.22)$$

$$S_0(x_t) = \frac{4x_t - 11x_t^2 + x_t^3}{4(1 - x_t)^2} - \frac{3x_t^3}{2(1 - x_t)^3} \log x_t, \quad (4.23)$$

$$S_0(x_c) = x_c, \quad (4.24)$$

$$S_0(x_t, x_c) = x_c \left(\log \frac{x_t}{x_c} - \frac{3x_t}{4(1 - x_t)} - \frac{3x_t^2}{4(1 - x_t)^2} \log x_t \right) \quad (4.25)$$

are the usual Inami Lim functions [66]. These results are in agreement with refs. [37, 39].³ Due to the presence of additional non SM-like diagrams, C_9 and C_{10} contain pieces that are not just scalings of the SM result:

$$C_9 = 2v^2 C_{Hq}^{(3)} \left(\frac{4s_\theta^2 - 1}{s_\theta^2} I^{Hq3}(x_t) - \frac{1}{s_\theta^2} B_0(x_t) - D_0(x_t) \right), \quad (4.26)$$

$$C_{10} = 2v^2 C_{Hq}^{(3)} \frac{1}{s_\theta^2} (B_0(x_t) + I^{Hq3}(x_t)), \quad (4.27)$$

where

$$I^{Hq3}(x_t) = \frac{x_t}{32} \left[-7 \log \frac{m_W^2}{\mu^2} + \frac{x_t + 33}{2(1 - x_t)} - \frac{7x_t^2 - 2x_t + 12}{(1 - x_t)^2} \log x_t \right], \quad (4.28)$$

and

$$B_0(x_t) = \frac{1}{4} \left[\frac{x_t}{1 - x_t} + \frac{x_t}{(x_t - 1)^2} \log x_t \right], \quad (4.29)$$

$$C_0(x_t) = \frac{x_t}{8} \left[\frac{x_t - 6}{x_t - 1} + \frac{3x_t + 2}{(x_t - 1)^2} \log x_t \right], \quad (4.30)$$

$$D_0(x_t) = -\frac{4}{9} \log x_t + \frac{-19x_t^3 + 25x_t^2}{36(x_t - 1)^3} + \frac{x_t^2(5x_t^2 - 2x_t - 6)}{18(x_t - 1)^4} \log x_t \quad (4.31)$$

are again the usual Inami Lim [66] functions.⁴

³Our results are in fact twice theirs; however this is accounted for by a slight difference in operator flavour structure. They study an operator containing a b quark (without corresponding contributions for the first two generations), and hence only half of the charged current vertices of these diagrams can be affected by the operator; by contrast in our flavour structure all charged current vertices can be affected.

⁴Note that the functions $I^{Hq3}(x_t)$, $B_0(x_t)$, $C_0(x_t)$ and $D_0(x_t)$ are individually gauge parameter ξ dependent, and are given here in Feynman gauge. The overall result is of course ξ -independent.

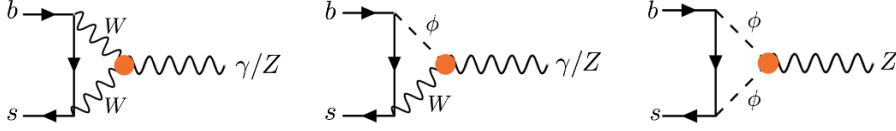


Figure 8. Diagrams generating contributions to $b \rightarrow sl^+l^-$ and/or $b \rightarrow s\gamma$ from Q_W (first diagram only), Q_{HD} (second and third diagrams only), and Q_{HWB} (all three diagrams). Since the operators Q_{HD} and Q_{HWB} affect the Z mass, and Q_{HWB} affects the Z and photon couplings by redefining the Weinberg angle, SM-like penguin diagrams also receive contributions from these operators and are included in our calculation.

4.6 Q_W

This operator produces a triple gauge boson vertex with a different Lorentz structure to those in the SM, and generates contributions to $b \rightarrow sl^+l^-$ and $b \rightarrow s\gamma$ via the first diagram in figure 8. These are

$$C_7 = \frac{3}{2}g_2v^2C_W \left(-\frac{x_t^2 + x_t}{2(x_t - 1)^2} + \frac{x_t^2}{(x_t - 1)^3} \log x_t \right), \quad (4.32)$$

$$C_9 = \frac{3}{2}g_2v^2C_W \left(\frac{3x_t^2 - x_t}{2(x_t - 1)^2} - \frac{x_t^3}{(x_t - 1)^3} \log x_t \right). \quad (4.33)$$

Our result agrees with ref. [42] (accounting for a difference in normalisation between their operator O_{3W} and our operator Q_W).

4.7 Q_{HWB}

This operator redefines the Weinberg angle (and hence enters γ/Z vertices), but also induces new bosonic couplings with a different Lorentz structure to those in the SM, directly generating contributions to $b \rightarrow s\gamma$ and $b \rightarrow sl^+l^-$ via the diagrams in figure 8. In total we get

$$C_7 = -v^2C_{HWB} \frac{g_2}{g_1} \left(\frac{8x_t^2 - 7x_t + 5}{24(1 - x_t)^3} + \frac{x_t(x_t^2 - x_t + 1)}{4(1 - x_t)^4} \log x_t \right), \quad (4.34)$$

$$C_9 = v^2C_{HWB} \frac{g_2}{g_1} \left(\frac{x_t(-9x_t^3 + 100x_t^2 - 178x_t + 81)}{18(1 - x_t)^3} + \frac{39x_t^4 - 30x_t^3 - 81x_t^2 + 82x_t - 16}{18(1 - x_t)^4} \log x_t \right). \quad (4.35)$$

4.8 Q_{HD}

The operator Q_{HD} enters in the definition of theory parameters, notably m_Z and the Z couplings, due to its correction of the Higgs kinetic term; it also directly generates contributions to $b \rightarrow sl^+l^-$ via the last two diagrams in figure 8. In total, the contributions

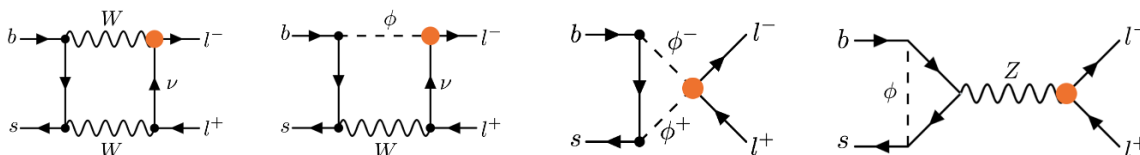


Figure 9. Diagrams generating contributions to $b \rightarrow sl^+l^-$ from the operator $Q_{Hl}^{(3)}$. The first two diagrams should be taken to include also similar diagrams with the effective operator attaching to the l^+ line rather than the l^- line, while the fourth diagram should be taken to include all other Z penguin diagrams (including those with self-energies on external legs) where these operators affect the Zl^+l^- vertex.

from this operator are

$$C_7 = \frac{1}{8} \frac{v^2}{s_\theta^2} C_{HD} (1 - s_\theta^2) D'_0(x_t), \quad (4.36)$$

$$C_9 = \frac{1}{2} \frac{v^2}{s_\theta^2} C_{HD} \left[(1 - 4s_\theta^2) I(x_t) + (1 - s_\theta^2) (D_0(x_t) + 4C_0(x_t)) \right], \quad (4.37)$$

$$C_{10} = -\frac{1}{2} \frac{v^2}{s_\theta^2} C_{HD} I(x_t), \quad (4.38)$$

where $D'_0(x_t)$, $C_0(x_t)$ and $D_0(x_t)$ are the usual Inami Lim functions defined in eqs. (4.21), (4.30) and (4.31), and $I(x_t)$ has been defined in eq. (4.10).

4.9 $Q_{Hl}^{(3)}$ and Q_u

These operators enter every electroweak process since they are involved in the definition of G_F , which we take as an input parameter. The $Q_{Hl}^{(3)}$ operator also generates direct contributions to the $b \rightarrow sl^+l^-$ process, as shown in figure 9. As described in section 2, there are two ways of contracting the lepton doublets within Q_u to make a flavour singlet, so we can define two independent Wilson coefficients, C_u and C'_u , within our $U(3)^5$ invariant theory, although only C'_u contributes here. Then the matching results for these operators are

$$C_{1,\text{mix}}^s(x_t) = -4v^2 \left(C_{Hl}^{(3)} - \frac{1}{2} C'_u \right) S_0(x_t), \quad (4.39)$$

$$C_{1,\text{mix}}^s(x_c) = -4v^2 \left(C_{Hl}^{(3)} - \frac{1}{2} C'_u \right) S_0(x_c), \quad (4.40)$$

$$C_{1,\text{mix}}^s(x_t, x_c) = -4v^2 \left(C_{Hl}^{(3)} - \frac{1}{2} C'_u \right) S_0(x_t, x_c), \quad (4.41)$$

$$C_7 = \frac{3}{2} v^2 \left(C_{Hl}^{(3)} - \frac{1}{2} C'_u \right) D'_0(x_t), \quad (4.42)$$

$$C_8 = v^2 \left(C_{Hl}^{(3)} - \frac{1}{2} C'_u \right) E'_0(x_t), \quad (4.43)$$

$$C_9 = -4v^2 \left(C_{Hl}^{(3)} - \frac{1}{2} C'_u \right) \left(\frac{(1 - 4s_\theta^2)}{s_\theta^2} C_0(x_t) - \frac{1}{s_\theta^2} B_0(x_t) - D_0(x_t) \right) - \frac{v^2}{s_\theta^2} C_{Hl}^{(3)} I^{Hl3}(x_t), \quad (4.44)$$

$$C_{10} = -4v^2 \frac{1}{s_\theta^2} \left(C_{HI}^{(3)} - \frac{1}{2} C'_{II} \right) (B_0(x_t) - C_0(x_t)) + \frac{v^2}{s_\theta^2} C_{HI}^{(3)} I^{HI3}(x_t), \quad (4.45)$$

where

$$I^{HI3}(x_t) = \frac{x_t}{16} \left[\log \frac{m_W^2}{\mu^2} + \frac{7x_t - 25}{2(1-x_t)} + \frac{x_t^2 - 14x_t + 4}{(1-x_t)^2} \log x_t \right], \quad (4.46)$$

and the Inami Lim functions $B_0(x_t)$, $C_0(x_t)$, $D_0(x_t)$, $S_0(x_t)$, $S_0(x_c)$, $S_0(x_t, x_c)$, $D'_0(x_t)$ and $E'_0(x_t)$ were defined in eqs. (4.21)–(4.25) and (4.29)–(4.31).

5 Conclusions and outlook

We have calculated here for the first time the full tree and one-loop matching of the SMEFT in the limit of complete $U(3)^5$ flavour symmetry in the UV onto the operators of the WET which contribute to down-sector FCNCs. Having these available, it will now be straightforward to run them to the appropriate experimental scale within the WET⁵ and derive the constraints that flavour observables provide on this flavour-symmetric limit of the SMEFT. In a forthcoming publication, we shall explore these constraints and compare their sensitivity to those arising from other measurements sensitive to similar sets of Wilson coefficients, for example electroweak precision observables, including the effects of operators which are allowed at linear order in the MFV expansion. It is likely that these calculations will allow the derivation of constraints which lie in directions in parameter space linearly independent from those that currently exist from global fits to the flavour symmetric SMEFT.

Ultimately, only a truly global picture of the SMEFT parameter space can give us meaningful insight into the underlying structure of new physics. If hints of physics beyond the SM appear in upcoming experiments, an understanding of global constraints on effective operators will signpost the most promising explanations, while if no deviation from SM predictions is seen this global picture will allow constraints to be easily placed on as-yet unimagined new models. The absence of explicit flavour structure is largely required if new physics is to be accessible at near-future experiments, or is expected to play a meaningful role in resolving the gauge hierarchy problem; this work provides tools to put new constraints from flavour observables on these models.

Acknowledgments

We gratefully acknowledge multiple helpful exchanges with Ilaria Brivio and Christoph Greub. The research of WS was partially funded by the Alexander von Humboldt Foundation in the framework of the Sofja Kovalevskaja Award 2016, endowed by the German Federal Ministry of Education and Research. This work also was supported by the Cluster of Excellence ‘Precision Physics, Fundamental Interactions, and Structure of Matter’ (PRISMA+ EXC 2118/1) funded by the German Research Foundation (DFG) within the German Excellence Strategy (Project ID 39083149), as well as BMBF Verbundprojekt 05H2018 - Belle II: Indirekte Suche nach neuer Physik bei Belle-II. TH thanks the CERN

⁵Anomalous dimensions can be found in refs. [67, 68].

theory group for its hospitality during his regular visits to CERN where part of the work was done. SR is grateful to UCSB physics department and KITP Santa Barbara for hospitality while working on this.

A Input parameter dependence of results

As described in section 3, there is a choice to be made in the electroweak input parameters, which affects the pieces of the result which depend on the resulting dimension-six input parameter shifts δg_1 , δg_2 and δv . In the main text we have chosen to take the three measured electroweak input parameters as $\{\hat{m}_W, \hat{m}_Z, \hat{G}_F\}$. The purpose of this appendix is to clarify which pieces of our results are dependent on this choice, and to provide results for the alternative input scheme in which $\{\hat{\alpha}_{em}, \hat{m}_Z, \hat{G}_F\}$ are the set of measured electroweak inputs.

In the $\{\hat{m}_W, \hat{m}_Z, \hat{G}_F\}$ input scheme, the basis shifts are given by [69]

$$\frac{\delta g_1}{g_1} = v^2 \left(\left(-C_{Hl3} + \frac{1}{2} C'_{ll} \right) - \frac{1}{4g_1^2} (g_2^2 + g_1^2) C_{HD} - \frac{g_2}{g_1} C_{HWB} \right), \quad (\text{A.1})$$

$$\frac{\delta g_2}{g_2} = -v^2 \left(-\frac{1}{2} C'_{ll} + C_{Hl}^{(3)} \right), \quad (\text{A.2})$$

$$\frac{\delta v}{v} = v^2 \left(-\frac{1}{2} C'_{ll} + C_{Hl}^{(3)} \right), \quad (\text{A.3})$$

while in the $\{\hat{\alpha}_{em}, \hat{m}_Z, \hat{G}_F\}$ input scheme, the basis shifts are defined

$$\frac{\delta g_1}{g_1} = -\frac{g_1 v^2}{(g_1^2 - g_2^2)} \left(\frac{g_1}{4} C_{HD} + g_2 C_{HWB} \right), \quad (\text{A.4})$$

$$\frac{\delta g_2}{g_2} = \frac{g_2 v^2}{(g_1^2 - g_2^2)} \left(\frac{g_2}{4} C_{HD} + g_1 C_{HWB} \right), \quad (\text{A.5})$$

$$\frac{\delta v}{v} = v^2 \left(-\frac{1}{2} C'_{ll} + C_{Hl}^{(3)} \right). \quad (\text{A.6})$$

For the definitions of hatted parameters in the $\{\hat{\alpha}_{em}, \hat{m}_Z, \hat{G}_F\}$ input scheme in terms of the measured inputs, we refer to ref. [69]. In order to allow switching between the different schemes, our results can be written as shift-independent pieces (i.e. pieces that remain when all three δ s are set to zero) plus pieces written in terms of these three δ s. We emphasise that our results in the main text in section 4 are the sum of these pieces, for the $\{\hat{m}_W, \hat{m}_Z, \hat{G}_F\}$ input scheme. The shift-independent pieces and the shift-dependent pieces of our calculation are separately independent of the gauge parameter ξ , as they must be since the gauge-invariance of the SMEFT does not rely on the values of the Lagrangian parameters \bar{g}_1 , \bar{g}_2 , and \bar{v} .

In the next subsection, we present the shift-independent pieces (meaning, specifically, the results you get by performing only steps 1 and 2 of the procedure in section 3) for the three operators that also appear in the input shifts. Then we present the extra shift-dependent pieces that should be added to these in the $\{\hat{m}_W, \hat{m}_Z, \hat{G}_F\}$ scheme (section A.2) or in the $\{\hat{\alpha}_{em}, \hat{m}_Z, \hat{G}_F\}$ scheme (section A.3). Note that the form of the corrections in the

first scheme, chosen for our main results presentation, is notably simpler than that in the second; this is due to the fact that m_W is a fundamental input in the first and a complicated derived quantity in the second, and m_W appears very often throughout these calculations.

A.1 Input shift independent pieces

The only SMEFT Wilson coefficients which appear in both the input shift pieces and the shift-independent pieces, for the two schemes given above, are $C_{HI}^{(3)}$, C_{HD} , and C_{HWB} . The coefficient C'_{ll} only contributes via input shifts. For all other Wilson coefficients, the results given in the main text are shift-independent.

A.1.1 $Q_{HI}^{(3)}$

$$C_9 = -v^2 C_{HI}^{(3)} \frac{1}{s_\theta^2} \frac{x_t}{16} \left(\log \frac{m_W^2}{\mu^2} + \frac{7x_t - 25}{2(1-x_t)} + \frac{x_t^2 - 14x_t + 4}{(1-x_t)^2} \log x_t \right), \quad (\text{A.7})$$

$$C_{10} = v^2 C_{HI}^{(3)} \frac{1}{s_\theta^2} \frac{x_t}{16} \left(\log \frac{m_W^2}{\mu^2} + \frac{7x_t - 25}{2(1-x_t)} + \frac{x_t^2 - 14x_t + 4}{(1-x_t)^2} \log x_t \right). \quad (\text{A.8})$$

A.1.2 Q_{HD}

$$C_9 = -\frac{1}{2} \frac{4s_\theta^2 - 1}{s_\theta^2} v^2 C_{HD} I(x_t), \quad (\text{A.9})$$

$$C_{10} = -\frac{1}{2} \frac{1}{s_\theta^2} v^2 C_{HD} I(x_t), \quad (\text{A.10})$$

where $I(x_t)$ is defined in eq. (4.10).

A.1.3 C_{HWB}

$$C_7 = v^2 C_{HWB} \frac{g_2}{g_1} \left(\frac{g_1^2 - g_2^2}{g_1^2 + g_2^2} \frac{1}{4} D'_0(x_t) + I_7^{HWB}(x_t) \right), \quad (\text{A.11})$$

$$C_9 = v^2 C_{HWB} \frac{g_2}{g_1} \left(\frac{g_1^2 - g_2^2}{g_1^2 + g_2^2} (4C_0(x_t) + D_0(x_t)) + I_9^{HWB}(x_t) \right), \quad (\text{A.12})$$

where

$$I_7^{HWB}(x_t) = -\frac{x_t(8x_t^2 - 19x_t + 17)}{48(1-x_t)^3} - \frac{x_t(2x_t^2 - 5x_t + 4)}{8(1-x_t)^4} \log x_t, \quad (\text{A.13})$$

$$I_9^{HWB}(x_t) = \frac{x_t(37x_t^2 - 97x_t + 54)}{36(1-x_t)^3} + \frac{15x_t^4 - 24x_t^3 - 18x_t^2 + 32x_t - 8}{18(1-x_t)^4} \log x_t, \quad (\text{A.14})$$

and $C_0(x_t)$, $D_0(x_t)$ and $D'_0(x_t)$ are the usual Inami Lim functions defined in eqs. (4.30), (4.31) and (4.21).

A.2 Input shift pieces for $\{\hat{m}_W, \hat{m}_Z, \hat{G}_F\}$ scheme

$$C_{1,\text{mix}}^s(x_t) = -4v^2 \left(C_{Hl}^{(3)} - \frac{1}{2} C'_{ll} \right) S_0(x_t), \quad (\text{A.15})$$

$$C_{1,\text{mix}}^s(x_c) = -4v^2 \left(C_{Hl}^{(3)} - \frac{1}{2} C'_{ll} \right) S_0(x_c), \quad (\text{A.16})$$

$$C_{1,\text{mix}}^s(x_t, x_c) = -4v^2 \left(C_{Hl}^{(3)} - \frac{1}{2} C'_{ll} \right) S_0(x_t, x_c), \quad (\text{A.17})$$

$$C_7 = v^2 \left[\frac{3}{2} \left(C_{Hl}^{(3)} - \frac{1}{2} C'_{ll} \right) + \frac{1}{2} \frac{g_2}{g_1} c_\theta^2 C_{HWB} + \frac{1}{8} \frac{g_2^2}{g_1^2} C_{HD} \right] D'_0(x_t), \quad (\text{A.18})$$

$$C_8 = v^2 \left(C_{Hl}^{(3)} - \frac{1}{2} C'_{ll} \right) E'_0(x_t), \quad (\text{A.19})$$

$$C_9 = -4v^2 \left(C_{Hl}^{(3)} - \frac{1}{2} C'_{ll} \right) \left(\frac{(1-4s_\theta^2)}{s_\theta^2} C_0(x_t) - \frac{1}{s_\theta^2} B_0(x_t) - D_0(x_t) \right) \\ + v^2 \left(2 \frac{g_2}{g_1} c_\theta^2 C_{HWB} + \frac{1}{2} \frac{g_2^2}{g_1^2} C_{HD} \right) (D_0(x_t) + 4C_0(x_t)), \quad (\text{A.20})$$

$$C_{10} = -4v^2 \frac{1}{s_\theta^2} \left(C_{Hl}^{(3)} - \frac{1}{2} C'_{ll} \right) (B_0(x_t) - C_0(x_t)), \quad (\text{A.21})$$

where $B_0(x_t)$, $C_0(x_t)$, $D_0(x_t)$, $D'_0(x_t)$, $E'_0(x_t)$, $S_0(x_t)$, $S_0(x_c)$ and $S_0(x_t, x_c)$ are the usual Inami Lim functions defined in eqs. (4.21)–(4.25) and (4.29)–(4.31).

A.3 Input shift pieces for $\{\hat{\alpha}_{em}, \hat{m}_Z, \hat{G}_F\}$ scheme

$$C_{1,\text{mix}}^s(x_t) = -4v^2 \left(C_{Hl}^{(3)} - \frac{1}{2} C'_{ll} \right) S_0(x_t), \quad (\text{A.22})$$

$$C_{1,\text{mix}}^s(x_c) = -4v^2 \left(C_{Hl}^{(3)} - \frac{1}{2} C'_{ll} \right) S_0(x_c), \quad (\text{A.23})$$

$$C_{1,\text{mix}}^s(x_t, x_c) = -4v^2 \left(C_{Hl}^{(3)} - \frac{1}{2} C'_{ll} \right) S_0(x_t, x_c), \quad (\text{A.24})$$

$$C_7 = v^2 \left(C_{Hl}^{(3)} - \frac{1}{2} C'_{ll} \right) \\ \times \left[\frac{x_t(2x_t^3 - 75x_t^2 - 66x_t + 67)}{72(1-x_t)^4} - \frac{x_t(3x_t^3 + 19x_t^2 - 6x_t - 4)}{12(1-x_t)^5} \log x_t \right] \\ - \frac{g_2^2 v^2}{(g_1^2 - g_2^2)} \left(\frac{1}{4} C_{HD} + \frac{g_1}{g_2} C_{HWB} \right) \left[\frac{x_t(46x_t^3 + 57x_t^2 - 6x_t - 25)}{72(1-x_t)^4} \right. \\ \left. + \frac{x_t(21x_t^3 - 11x_t^2 + 6x_t - 4)}{12(1-x_t)^5} \log x_t \right] - \frac{1}{2} \frac{g_1 g_2 v^2}{(g_1^2 + g_2^2)} C_{HWB} D'_0(x_t), \quad (\text{A.25})$$

$$C_8 = v^2 \left(C_{Hl}^{(3)} - \frac{1}{2} C'_{ll} \right) \left[-\frac{x_t(x_t^3 - 6x_t^2 - 15x_t - 16)}{12(1-x_t)^4} + \frac{x_t(2x_t^2 + 3x_t + 1)}{2(1-x_t)^5} \log x_t \right] \\ - \frac{g_2^2 v^2}{(g_1^2 - g_2^2)} \left(\frac{1}{4} C_{HD} + \frac{g_1}{g_2} C_{HWB} \right) \\ \times \left[\frac{x_t(2x_t^3 - 12x_t^2 - 3x_t - 5)}{6(1-x_t)^4} - \frac{x_t(5x_t^2 + 1)}{2(1-x_t)^5} \log x_t \right], \quad (\text{A.26})$$

1 : X^3		2 : H^6		3 : $H^4 D^2$		5 : $\psi^2 H^3 + \text{h.c.}$			
Q_G	$f^{ABC} G_\mu^{A\nu} G_\nu^{B\rho} G_\rho^{C\mu}$	Q_H	$(H^\dagger H)^3$	$Q_{H\Box}$	$(H^\dagger H)\Box(H^\dagger H)$	Q_{eH}	$(H^\dagger H)(\bar{l}_p e_r H)$		
$Q_{\tilde{G}}$	$f^{ABC} \tilde{G}_\mu^{A\nu} G_\nu^{B\rho} G_\rho^{C\mu}$			Q_{HD}	$(H^\dagger D_\mu H)^* (H^\dagger D_\mu H)$	Q_{uH}	$(H^\dagger H)(\bar{q}_p u_r \tilde{H})$	Q_{dH}	$(H^\dagger H)(\bar{q}_p d_r H)$
Q_W	$\epsilon^{IJK} W_\mu^{I\nu} W_\nu^{J\rho} W_\rho^{K\mu}$								
$Q_{\tilde{W}}$	$\epsilon^{IJK} \tilde{W}_\mu^{I\nu} W_\nu^{J\rho} W_\rho^{K\mu}$								
4 : $X^2 H^2$		6 : $\psi^2 XH + \text{h.c.}$		7 : $\psi^2 H^2 D$					
Q_{HG}	$H^\dagger H G_{\mu\nu}^A G^{A\mu\nu}$	Q_{eW}	$(\bar{l}_p \sigma^{\mu\nu} e_r) \tau^I H W_{\mu\nu}^I$	$Q_{Hl}^{(1)}$	$(H^\dagger i \overleftrightarrow{D}_\mu H)(\bar{l}_p \gamma^\mu l_r)$	$Q_{Hl}^{(3)}$	$(H^\dagger i \overleftrightarrow{D}_\mu^I H)(\bar{l}_p \tau^I \gamma^\mu l_r)$		
$Q_{H\tilde{G}}$	$H^\dagger H \tilde{G}_{\mu\nu}^A G^{A\mu\nu}$	Q_{eB}	$(\bar{l}_p \sigma^{\mu\nu} e_r) H B_{\mu\nu}$	Q_{He}	$(H^\dagger i \overleftrightarrow{D}_\mu H)(\bar{e}_p \gamma^\mu e_r)$	$Q_{Hq}^{(1)}$	$(H^\dagger i \overleftrightarrow{D}_\mu H)(\bar{q}_p \gamma^\mu q_r)$		
Q_{HW}	$H^\dagger H W_{\mu\nu}^I W^{I\mu\nu}$	Q_{uG}	$(\bar{q}_p \sigma^{\mu\nu} T^A u_r) \tilde{H} G_{\mu\nu}^A$	$Q_{Hq}^{(3)}$	$(H^\dagger i \overleftrightarrow{D}_\mu^I H)(\bar{q}_p \tau^I \gamma^\mu q_r)$	Q_{Hu}	$(H^\dagger i \overleftrightarrow{D}_\mu H)(\bar{u}_p \gamma^\mu u_r)$		
$Q_{H\tilde{W}}$	$H^\dagger H \tilde{W}_{\mu\nu}^I W^{I\mu\nu}$	Q_{uW}	$(\bar{q}_p \sigma^{\mu\nu} u_r) \tau^I \tilde{H} W_{\mu\nu}^I$	Q_{Hd}	$(H^\dagger i \overleftrightarrow{D}_\mu H)(\bar{d}_p \gamma^\mu d_r)$	$Q_{Hud} + \text{h.c.}$	$i(\tilde{H}^\dagger D_\mu H)(\bar{u}_p \gamma^\mu d_r)$		
Q_{HB}	$H^\dagger H B_{\mu\nu} B^{\mu\nu}$	Q_{uB}	$(\bar{q}_p \sigma^{\mu\nu} u_r) \tilde{H} B_{\mu\nu}$						
$Q_{H\tilde{B}}$	$H^\dagger H \tilde{B}_{\mu\nu} B^{\mu\nu}$	Q_{dG}	$(\bar{q}_p \sigma^{\mu\nu} T^A d_r) H G_{\mu\nu}^A$						
Q_{HWB}	$H^\dagger \tau^I H W_{\mu\nu}^I B^{\mu\nu}$	Q_{dW}	$(\bar{q}_p \sigma^{\mu\nu} d_r) \tau^I H W_{\mu\nu}^I$						
$Q_{H\tilde{W}B}$	$H^\dagger \tau^I H \tilde{W}_{\mu\nu}^I B^{\mu\nu}$	Q_{dB}	$(\bar{q}_p \sigma^{\mu\nu} d_r) H B_{\mu\nu}$						
8 : $(\bar{L}L)(\bar{L}L)$		8 : $(\bar{R}R)(\bar{R}R)$		8 : $(\bar{L}L)(\bar{R}R)$					
$Q_{\ell\ell}$	$(\bar{l}_p \gamma_\mu l_r)(\bar{l}_s \gamma^\mu l_t)$	Q_{ee}	$(\bar{e}_p \gamma_\mu e_r)(\bar{e}_s \gamma^\mu e_t)$	Q_{le}	$(\bar{l}_p \gamma_\mu l_r)(\bar{e}_s \gamma^\mu e_t)$				
$Q_{qq}^{(1)}$	$(\bar{q}_p \gamma_\mu q_r)(\bar{q}_s \gamma^\mu q_t)$	Q_{uu}	$(\bar{u}_p \gamma_\mu u_r)(\bar{u}_s \gamma^\mu u_t)$	Q_{lu}	$(\bar{l}_p \gamma_\mu l_r)(\bar{u}_s \gamma^\mu u_t)$				
$Q_{qq}^{(3)}$	$(\bar{q}_p \gamma_\mu \tau^I q_r)(\bar{q}_s \gamma^\mu \tau^I q_t)$	Q_{dd}	$(\bar{d}_p \gamma_\mu d_r)(\bar{d}_s \gamma^\mu d_t)$	Q_{ld}	$(\bar{l}_p \gamma_\mu l_r)(\bar{d}_s \gamma^\mu d_t)$				
$Q_{\ell q}^{(1)}$	$(\bar{l}_p \gamma_\mu l_r)(\bar{q}_s \gamma^\mu q_t)$	Q_{eu}	$(\bar{e}_p \gamma_\mu e_r)(\bar{u}_s \gamma^\mu u_t)$	Q_{qe}	$(\bar{q}_p \gamma_\mu q_r)(\bar{e}_s \gamma^\mu e_t)$				
$Q_{\ell q}^{(3)}$	$(\bar{l}_p \gamma_\mu \tau^I l_r)(\bar{q}_s \gamma^\mu \tau^I q_t)$	Q_{ed}	$(\bar{e}_p \gamma_\mu e_r)(\bar{d}_s \gamma^\mu d_t)$	$Q_{qu}^{(1)}$	$(\bar{q}_p \gamma_\mu q_r)(\bar{u}_s \gamma^\mu u_t)$				
		$Q_{ud}^{(1)}$	$(\bar{u}_p \gamma_\mu u_r)(\bar{d}_s \gamma^\mu d_t)$	$Q_{qu}^{(8)}$	$(\bar{q}_p \gamma_\mu T^A q_r)(\bar{u}_s \gamma^\mu T^A u_t)$				
		$Q_{ud}^{(8)}$	$(\bar{u}_p \gamma_\mu T^A u_r)(\bar{d}_s \gamma^\mu T^A d_t)$	$Q_{qd}^{(1)}$	$(\bar{q}_p \gamma_\mu q_r)(\bar{d}_s \gamma^\mu d_t)$				
				$Q_{qd}^{(8)}$	$(\bar{q}_p \gamma_\mu T^A q_r)(\bar{d}_s \gamma^\mu T^A d_t)$				
8 : $(\bar{L}R)(\bar{R}L) + \text{h.c.}$		8 : $(\bar{L}R)(\bar{L}R) + \text{h.c.}$							
Q_{ledq}	$(\bar{l}_p^j e_r)(\bar{d}_s^k q_t^j)$	$Q_{quqd}^{(1)}$	$(\bar{q}_p^j u_r) \epsilon_{jk} (\bar{q}_s^k d_t)$						
		$Q_{quqd}^{(8)}$	$(\bar{q}_p^j T^A u_r) \epsilon_{jk} (\bar{q}_s^k T^A d_t)$						
		$Q_{lequ}^{(1)}$	$(\bar{l}_p^j e_r) \epsilon_{jk} (\bar{q}_s^k u_t)$						
		$Q_{lequ}^{(3)}$	$(\bar{l}_p^j \sigma_{\mu\nu} e_r) \epsilon_{jk} (\bar{q}_s^k \sigma^{\mu\nu} u_t)$						

Table 3. The independent dimension-six operators built from Standard Model fields which conserve baryon number, as given in ref. [9]. The flavour labels p, r, s, t on the Q operators are suppressed on the left hand side of the tables.

$$\begin{aligned}
C_9 = & v^2 \left(C_{Hl}^{(3)} - \frac{1}{2} C'_{ll} \right) \left[-\frac{1}{s_\theta^2} \left(\frac{x_t(x_t^2 - 2x_t + 4)}{2(1-x_t)^2} - \frac{3x_t^2(x_t - 3)}{4(1-x_t)^3} \log x_t \right) \right. \\
& + \frac{x_t(108x_t^4 - 530x_t^3 + 1557x_t^2 - 1908x_t + 737)}{54(1-x_t)^4} \\
& \left. - \frac{24x_t^5 - 126x_t^4 + 123x_t^3 + 35x_t^2 - 54x_t + 4}{9(1-x_t)^5} \log x \right] \\
& + \frac{g_2^2 v^2}{(g_1^2 - g_2^2)} \left(\frac{1}{4} C_{HD} + \frac{g_1}{g_2} C_{HWB} \right) \left[\frac{x_t(54x_t^4 - 149x_t^3 + 615x_t^2 - 969x_t + 413)}{54(1-x_t)^4} \right. \\
& \left. - \frac{27x_t^5 - 219x_t^4 + 333x_t^3 - 129x_t^2 + 8x_t - 8}{18(1-x_t)^5} \log x_t \right] \\
& + \frac{g_2^2}{g_1^2} v^2 \left(\frac{1}{4} C_{HD} + \frac{g_1}{g_2} C_{HWB} \right) \left(\frac{3x_t^2}{2(1-x_t)^2} + \frac{3x_t^2(1+x_t)}{4(1-x_t)^3} \log x_t \right) \\
& - 2 \frac{g_1 g_2 v^2}{g_1^2 + g_2^2} C_{HWB} (4C_0(x_t) + D_0(x_t)), \tag{A.27}
\end{aligned}$$

$$\begin{aligned}
C_{10} = & \frac{v^2}{s_\theta^2} \left(C_{Hl}^{(3)} - \frac{1}{2} C'_{ll} \right) \left[\frac{x_t(x_t^2 - 2x_t + 4)}{2(1-x_t)^2} - \frac{3x_t^2(x_t - 3)}{4(1-x_t)^3} \log x_t \right] \tag{A.28} \\
& + \frac{1}{s_\theta^2} \frac{g_2^2 v^2}{(g_1^2 - g_2^2)} \left(\frac{1}{4} C_{HD} + \frac{g_1}{g_2} C_{HWB} \right) \left[\frac{3x_t^2}{2(1-x_t)^2} + \frac{3x_t^2(x_t + 1)}{4(1-x_t)^3} \log x_t \right],
\end{aligned}$$

where $B_0(x_t)$, $C_0(x_t)$, $D_0(x_t)$, $D'_0(x_t)$, $E'_0(x_t)$, $S_0(x_t)$, $S_0(x_c)$ and $S_0(x_t, x_c)$ are the usual Inami Lim functions defined in eqs. (4.21)–(4.25) and (4.29)–(4.31).

Open Access. This article is distributed under the terms of the Creative Commons Attribution License ([CC-BY 4.0](https://creativecommons.org/licenses/by/4.0/)), which permits any use, distribution and reproduction in any medium, provided the original author(s) and source are credited.

References

- [1] ATLAS collaboration, *Observation of a new particle in the search for the Standard Model Higgs boson with the ATLAS detector at the LHC*, *Phys. Lett. B* **716** (2012) 1 [[arXiv:1207.7214](https://arxiv.org/abs/1207.7214)] [[INSPIRE](#)].
- [2] CMS collaboration, *Observation of a new boson at a mass of 125 GeV with the CMS experiment at the LHC*, *Phys. Lett. B* **716** (2012) 30 [[arXiv:1207.7235](https://arxiv.org/abs/1207.7235)] [[INSPIRE](#)].
- [3] ATLAS collaboration, *Combined measurements of Higgs boson production and decay using up to 80 fb⁻¹ of proton-proton collision data at $\sqrt{s} = 13$ TeV collected with the ATLAS experiment*, [ATLAS-CONF-2018-031](#), CERN, Geneva, Switzerland (2018).
- [4] CMS collaboration, *Combined measurements of Higgs boson couplings in proton-proton collisions at $\sqrt{s} = 13$ TeV*, *Eur. Phys. J. C* **79** (2019) 421 [[arXiv:1809.10733](https://arxiv.org/abs/1809.10733)] [[INSPIRE](#)].
- [5] I. Brivio and M. Trott, *The Standard Model as an effective field theory*, *Phys. Rept.* **793** (2019) 1 [[arXiv:1706.08945](https://arxiv.org/abs/1706.08945)] [[INSPIRE](#)].
- [6] J.C. Criado, *MatchingTools: a Python library for symbolic effective field theory calculations*, *Comput. Phys. Commun.* **227** (2018) 42 [[arXiv:1710.06445](https://arxiv.org/abs/1710.06445)] [[INSPIRE](#)].

- [7] S. Das Bakshi, J. Chakraborty and S.K. Patra, *CoDEx: Wilson coefficient calculator connecting SMEFT to UV theory*, *Eur. Phys. J. C* **79** (2019) 21 [[arXiv:1808.04403](#)] [[INSPIRE](#)].
- [8] J. Aebischer et al., *WCxf: an exchange format for Wilson coefficients beyond the Standard Model*, *Comput. Phys. Commun.* **232** (2018) 71 [[arXiv:1712.05298](#)] [[INSPIRE](#)].
- [9] B. Grzadkowski, M. Iskrzynski, M. Misiak and J. Rosiek, *Dimension-six terms in the Standard Model Lagrangian*, *JHEP* **10** (2010) 085 [[arXiv:1008.4884](#)] [[INSPIRE](#)].
- [10] E.E. Jenkins, A.V. Manohar and M. Trott, *Renormalization group evolution of the Standard Model dimension six operators I: formalism and lambda dependence*, *JHEP* **10** (2013) 087 [[arXiv:1308.2627](#)] [[INSPIRE](#)].
- [11] E.E. Jenkins, A.V. Manohar and M. Trott, *Renormalization group evolution of the Standard Model dimension six operators II: Yukawa dependence*, *JHEP* **01** (2014) 035 [[arXiv:1310.4838](#)] [[INSPIRE](#)].
- [12] R. Alonso, E.E. Jenkins, A.V. Manohar and M. Trott, *Renormalization group evolution of the Standard Model dimension six operators III: gauge coupling dependence and phenomenology*, *JHEP* **04** (2014) 159 [[arXiv:1312.2014](#)] [[INSPIRE](#)].
- [13] Z. Han and W. Skiba, *Effective theory analysis of precision electroweak data*, *Phys. Rev. D* **71** (2005) 075009 [[hep-ph/0412166](#)] [[INSPIRE](#)].
- [14] L. Berthier and M. Trott, *Towards consistent electroweak precision data constraints in the SMEFT*, *JHEP* **05** (2015) 024 [[arXiv:1502.02570](#)] [[INSPIRE](#)].
- [15] L. Berthier and M. Trott, *Consistent constraints on the Standard Model effective field theory*, *JHEP* **02** (2016) 069 [[arXiv:1508.05060](#)] [[INSPIRE](#)].
- [16] M. Bjørn and M. Trott, *Interpreting W mass measurements in the SMEFT*, *Phys. Lett. B* **762** (2016) 426 [[arXiv:1606.06502](#)] [[INSPIRE](#)].
- [17] L. Berthier, M. Bjørn and M. Trott, *Incorporating doubly resonant W^\pm data in a global fit of SMEFT parameters to lift flat directions*, *JHEP* **09** (2016) 157 [[arXiv:1606.06693](#)] [[INSPIRE](#)].
- [18] J. Ellis, C.W. Murphy, V. Sanz and T. You, *Updated global SMEFT fit to Higgs, diboson and electroweak data*, *JHEP* **06** (2018) 146 [[arXiv:1803.03252](#)] [[INSPIRE](#)].
- [19] E. da Silva Almeida, A. Alves, N. Rosa Agostinho, O.J.P. Éboli and M.C. Gonzalez-Garcia, *Electroweak sector under scrutiny: a combined analysis of LHC and electroweak precision data*, *Phys. Rev. D* **99** (2019) 033001 [[arXiv:1812.01009](#)] [[INSPIRE](#)].
- [20] C. Zhang and F. Maltoni, *Top-quark decay into Higgs boson and a light quark at next-to-leading order in QCD*, *Phys. Rev. D* **88** (2013) 054005 [[arXiv:1305.7386](#)] [[INSPIRE](#)].
- [21] R. Gauld, B.D. Pecjak and D.J. Scott, *One-loop corrections to $h \rightarrow b\bar{b}$ and $h \rightarrow \tau\bar{\tau}$ decays in the Standard Model dimension-6 EFT: four-fermion operators and the large- m_t limit*, *JHEP* **05** (2016) 080 [[arXiv:1512.02508](#)] [[INSPIRE](#)].
- [22] C. Hartmann and M. Trott, *On one-loop corrections in the Standard Model effective field theory; the $\Gamma(h \rightarrow \gamma\gamma)$ case*, *JHEP* **07** (2015) 151 [[arXiv:1505.02646](#)] [[INSPIRE](#)].
- [23] R. Gauld, B.D. Pecjak and D.J. Scott, *QCD radiative corrections for $h \rightarrow b\bar{b}$ in the Standard Model dimension-6 EFT*, *Phys. Rev. D* **94** (2016) 074045 [[arXiv:1607.06354](#)] [[INSPIRE](#)].

- [24] F. Maltoni, E. Vryonidou and C. Zhang, *Higgs production in association with a top-antitop pair in the Standard Model effective field theory at NLO in QCD*, *JHEP* **10** (2016) 123 [[arXiv:1607.05330](#)] [[INSPIRE](#)].
- [25] C. Zhang, *Single top production at next-to-leading order in the Standard Model effective field theory*, *Phys. Rev. Lett.* **116** (2016) 162002 [[arXiv:1601.06163](#)] [[INSPIRE](#)].
- [26] C. Hartmann, W. Shepherd and M. Trott, *The Z decay width in the SMEFT: y_t and λ corrections at one loop*, *JHEP* **03** (2017) 060 [[arXiv:1611.09879](#)] [[INSPIRE](#)].
- [27] J. Baglio, S. Dawson and I.M. Lewis, *An NLO QCD effective field theory analysis of W^+W^- production at the LHC including fermionic operators*, *Phys. Rev. D* **96** (2017) 073003 [[arXiv:1708.03332](#)] [[INSPIRE](#)].
- [28] S. Dawson and P.P. Giardino, *Higgs decays to ZZ and $Z\gamma$ in the Standard Model effective field theory: an NLO analysis*, *Phys. Rev. D* **97** (2018) 093003 [[arXiv:1801.01136](#)] [[INSPIRE](#)].
- [29] S. Dawson and A. Ismail, *Standard Model EFT corrections to Z boson decays*, *Phys. Rev. D* **98** (2018) 093003 [[arXiv:1808.05948](#)] [[INSPIRE](#)].
- [30] E. Vryonidou and C. Zhang, *Dimension-six electroweak top-loop effects in Higgs production and decay*, *JHEP* **08** (2018) 036 [[arXiv:1804.09766](#)] [[INSPIRE](#)].
- [31] S. Dawson and P.P. Giardino, *Electroweak corrections to Higgs boson decays to $\gamma\gamma$ and W^+W^- in Standard Model EFT*, *Phys. Rev. D* **98** (2018) 095005 [[arXiv:1807.11504](#)] [[INSPIRE](#)].
- [32] S. Dawson, P.P. Giardino and A. Ismail, *Standard Model EFT and the Drell-Yan process at high energy*, *Phys. Rev. D* **99** (2019) 035044 [[arXiv:1811.12260](#)] [[INSPIRE](#)].
- [33] S. Alte, M. König and W. Shepherd, *Consistent searches for SMEFT effects in non-resonant dijet events*, *JHEP* **01** (2018) 094 [[arXiv:1711.07484](#)] [[INSPIRE](#)].
- [34] S. Alte, M. König and W. Shepherd, *Consistent searches for SMEFT effects in non-resonant dilepton events*, [arXiv:1812.07575](#) [[INSPIRE](#)].
- [35] B. Grzadkowski and M. Misiak, *Anomalous Wtb coupling effects in the weak radiative B-meson decay*, *Phys. Rev. D* **78** (2008) 077501 [*Erratum ibid.* **D 84** (2011) 059903] [[arXiv:0802.1413](#)] [[INSPIRE](#)].
- [36] J.P. Lee and K.Y. Lee, *$B_d-\bar{B}_d$ mixing versus $B_s-\bar{B}_s$ mixing with the anomalous Wtb couplings*, [arXiv:0809.0751](#) [[INSPIRE](#)].
- [37] J. Drobnak, S. Fajfer and J.F. Kamenik, *Interplay of $t \rightarrow bW$ decay and B_q meson mixing in minimal flavor violating models*, *Phys. Lett. B* **701** (2011) 234 [[arXiv:1102.4347](#)] [[INSPIRE](#)].
- [38] J.F. Kamenik, M. Papucci and A. Weiler, *Constraining the dipole moments of the top quark*, *Phys. Rev. D* **85** (2012) 071501 [*Erratum ibid.* **D 88** (2013) 039903] [[arXiv:1107.3143](#)] [[INSPIRE](#)].
- [39] J. Drobnak, S. Fajfer and J.F. Kamenik, *Probing anomalous tWb interactions with rare B decays*, *Nucl. Phys. B* **855** (2012) 82 [[arXiv:1109.2357](#)] [[INSPIRE](#)].
- [40] R. Alonso, B. Grinstein and J. Martin Camalich, *SU(2) \times U(1) gauge invariance and the shape of new physics in rare B decays*, *Phys. Rev. Lett.* **113** (2014) 241802 [[arXiv:1407.7044](#)] [[INSPIRE](#)].

- [41] J. Brod, A. Greljo, E. Stamou and P. Uttayarat, *Probing anomalous $t\bar{t}Z$ interactions with rare meson decays*, *JHEP* **02** (2015) 141 [[arXiv:1408.0792](#)] [[INSPIRE](#)].
- [42] C. Bobeth and U. Haisch, *Anomalous triple gauge couplings from B -meson and kaon observables*, *JHEP* **09** (2015) 018 [[arXiv:1503.04829](#)] [[INSPIRE](#)].
- [43] J. Aebischer, A. Crivellin, M. Fael and C. Greub, *Matching of gauge invariant dimension-six operators for $b \rightarrow s$ and $b \rightarrow c$ transitions*, *JHEP* **05** (2016) 037 [[arXiv:1512.02830](#)] [[INSPIRE](#)].
- [44] V. Cirigliano, W. Dekens, J. de Vries and E. Mereghetti, *Constraining the top-Higgs sector of the Standard Model effective field theory*, *Phys. Rev. D* **94** (2016) 034031 [[arXiv:1605.04311](#)] [[INSPIRE](#)].
- [45] M. González-Alonso and J. Martin Camalich, *Global effective-field-theory analysis of new-physics effects in (semi)leptonic kaon decays*, *JHEP* **12** (2016) 052 [[arXiv:1605.07114](#)] [[INSPIRE](#)].
- [46] F. Feruglio, P. Paradisi and A. Pattori, *Revisiting lepton flavor universality in B decays*, *Phys. Rev. Lett.* **118** (2017) 011801 [[arXiv:1606.00524](#)] [[INSPIRE](#)].
- [47] F. Feruglio, P. Paradisi and A. Pattori, *On the importance of electroweak corrections for B anomalies*, *JHEP* **09** (2017) 061 [[arXiv:1705.00929](#)] [[INSPIRE](#)].
- [48] M. Bordone, G. Isidori and S. Trifinopoulos, *Semileptonic B -physics anomalies: a general EFT analysis within $U(2)^n$ flavor symmetry*, *Phys. Rev. D* **96** (2017) 015038 [[arXiv:1702.07238](#)] [[INSPIRE](#)].
- [49] C. Bobeth, A.J. Buras, A. Celis and M. Jung, *Yukawa enhancement of Z -mediated new physics in $\Delta S = 2$ and $\Delta B = 2$ processes*, *JHEP* **07** (2017) 124 [[arXiv:1703.04753](#)] [[INSPIRE](#)].
- [50] A. Celis, J. Fuentes-Martin, A. Vicente and J. Virto, *Gauge-invariant implications of the $LHCb$ measurements on lepton-flavor nonuniversality*, *Phys. Rev. D* **96** (2017) 035026 [[arXiv:1704.05672](#)] [[INSPIRE](#)].
- [51] D. Buttazzo, A. Greljo, G. Isidori and D. Marzocca, *B -physics anomalies: a guide to combined explanations*, *JHEP* **11** (2017) 044 [[arXiv:1706.07808](#)] [[INSPIRE](#)].
- [52] C. Cornella, F. Feruglio and P. Paradisi, *Low-energy effects of lepton flavour universality violation*, *JHEP* **11** (2018) 012 [[arXiv:1803.00945](#)] [[INSPIRE](#)].
- [53] D.M. Straub, *flavio: a Python package for flavour and precision phenomenology in the Standard Model and beyond*, [arXiv:1810.08132](#) [[INSPIRE](#)].
- [54] M. Endo, T. Kitahara and D. Ueda, *SMEFT top-quark effects on $\Delta F = 2$ observables*, [arXiv:1811.04961](#) [[INSPIRE](#)].
- [55] L. Silvestrini and M. Valli, *Model-independent bounds on the Standard Model effective theory from flavour physics*, [arXiv:1812.10913](#) [[INSPIRE](#)].
- [56] S. Descotes-Genon, A. Falkowski, M. Fedele, M. González-Alonso and J. Virto, *The CKM parameters in the SMEFT*, [arXiv:1812.08163](#) [[INSPIRE](#)].
- [57] J. Aebischer, J. Kumar, P. Stangl and D.M. Straub, *A global likelihood for precision constraints and flavour anomalies*, [arXiv:1810.07698](#) [[INSPIRE](#)].
- [58] A. Celis, J. Fuentes-Martin, A. Vicente and J. Virto, *DsixTools: the Standard Model effective field theory toolkit*, *Eur. Phys. J. C* **77** (2017) 405 [[arXiv:1704.04504](#)] [[INSPIRE](#)].

- [59] J. Aebischer, J. Kumar and D.M. Straub, *Wilson: a Python package for the running and matching of Wilson coefficients above and below the electroweak scale*, *Eur. Phys. J. C* **78** (2018) 1026 [[arXiv:1804.05033](#)] [[INSPIRE](#)].
- [60] G. D'Ambrosio, G.F. Giudice, G. Isidori and A. Strumia, *Minimal flavor violation: an effective field theory approach*, *Nucl. Phys. B* **645** (2002) 155 [[hep-ph/0207036](#)] [[INSPIRE](#)].
- [61] I. Brivio and M. Trott, *Scheming in the SMEFT... And a reparameterization invariance!*, *JHEP* **07** (2017) 148 [*Addendum ibid.* **05** (2018) 136] [[arXiv:1701.06424](#)] [[INSPIRE](#)].
- [62] C.P. Burgess, S. Godfrey, H. Konig, D. London and I. Maksymyk, *Model independent global constraints on new physics*, *Phys. Rev. D* **49** (1994) 6115 [[hep-ph/9312291](#)] [[INSPIRE](#)].
- [63] A. Falkowski and F. Riva, *Model-independent precision constraints on dimension-6 operators*, *JHEP* **02** (2015) 039 [[arXiv:1411.0669](#)] [[INSPIRE](#)].
- [64] A. Dedes, W. Materkowska, M. Paraskevas, J. Rosiek and K. Suxho, *Feynman rules for the Standard Model effective field theory in R_ξ -gauges*, *JHEP* **06** (2017) 143 [[arXiv:1704.03888](#)] [[INSPIRE](#)].
- [65] G. Buchalla, A.J. Buras and M.E. Lautenbacher, *Weak decays beyond leading logarithms*, *Rev. Mod. Phys.* **68** (1996) 1125 [[hep-ph/9512380](#)] [[INSPIRE](#)].
- [66] T. Inami and C.S. Lim, *Effects of superheavy quarks and leptons in low-energy weak processes $K_L \rightarrow \mu\bar{\mu}$, $K^+ \rightarrow \pi^+\nu\bar{\nu}$ and $K^0 \leftrightarrow \bar{K}^0$* , *Prog. Theor. Phys.* **65** (1981) 297 [*Erratum ibid.* **65** (1981) 1772] [[INSPIRE](#)].
- [67] E.E. Jenkins, A.V. Manohar and P. Stoffer, *Low-energy effective field theory below the electroweak scale: anomalous dimensions*, *JHEP* **01** (2018) 084 [[arXiv:1711.05270](#)] [[INSPIRE](#)].
- [68] J. Aebischer, M. Fael, C. Greub and J. Virto, *B physics beyond the Standard Model at one loop: complete renormalization group evolution below the electroweak scale*, *JHEP* **09** (2017) 158 [[arXiv:1704.06639](#)] [[INSPIRE](#)].
- [69] I. Brivio, Y. Jiang and M. Trott, *The SMEFTsim package, theory and tools*, *JHEP* **12** (2017) 070 [[arXiv:1709.06492](#)] [[INSPIRE](#)].